



Detecting and tracking eddies in oceanic flow fields: A vorticity based Euler-Lagrangian method

Rahel Vortmeyer-Kley¹, Ulf Gräwe^{2, 3}, and Ulrike Feudel¹

¹Institute for Chemistry and Biology of the Marine Environment, Theoretical Physics/Complex Systems, Carl von Ossietzky University Oldenburg, Oldenburg, Germany

²Leibniz Institute for Baltic Sea Research, Rostock-Warnemünde, Germany

³Institute of Meteorology and Climatology, Leibniz University Hannover, Hannover, Germany

Correspondence to: Rahel Vortmeyer-Kley (rahel.vortmeyer-kley@uni-oldenburg.de)

Abstract. Since eddies play a major role in the dynamics of oceanic flows, it is of great interest to detect them and gain information about their tracks, their lifetimes and their shapes. We develop a vorticity based heuristic Euler-Lagrangian descriptor utilizing the idea of Lagrangian coherent structures. In our approach we define an eddy as a region around an elliptic fixed point (eddy core) surrounded by manifolds (eddy boundaries). We test the performance of an eddy tracking tool based on this Euler-Lagrangian descriptor using a convection flow of four eddies, a synthetic vortex street and an eddy seeded model. The results for eddy lifetime and eddy shape are compared to the results obtained with the Okubo-Weiss parameter, the modulus of vorticity and an eddy tracking tool used in oceanography. We show that the Euler-Lagrangian descriptor estimates lifetimes closer to the analytical results than any other method. Furthermore we demonstrate that eddy tracking based on this descriptor is robust with respect to certain types of noise which makes it a suitable tool for eddy detection in velocity fields obtained from observation.

1 Introduction

Transport of particles and chemical substances mediated by hydrodynamic flows are important components in the dynamics of ocean and atmosphere. For this reason there is an increasing interest in identifying particular structures in the flows such as eddies or transport barriers to understand their role in transport and mixing of the fluid as well as their impact on e.g. marine biology. Of particular interest in oceanography are eddies, which can be responsible for the confinement of plankton within them and hence, important for the development of plankton blooms (Abraham (1998); Martin et al. (2002); Sandulescu et al. (2007)). Such eddies possess a large variety of sizes and lifetimes. To tackle the problem of recognizing such eddies in aperiodic flows, different approaches have been developed: on the one hand, there are several methods available which are inspired by dynamical systems theory (Haller (2015)), on the other hand, numerical software for automated eddy detection has been developed in oceanography based on either physical quantities of the flow (Okubo (1970); Weiss (1991)) or geometric measures (Sadarjoen and Post (2000)).

Algorithms for finding eddies in fluid flows are applied in very different fields of science such as in atmospheric science (Koh and Legras (2002)), celestial mechanics (Gawlik et al. (2009)), biological oceanography (Bastine and Feudel (2010); Huhn et al.



(2012)) and the dynamics of swimmers (Wilson et al. (2009)). The largest field of application is oceanography, since oceanic flows contain a large number of mesoscale eddies of size 100-200 km, which are important components of advective transport. Their emergence and lifetime influences the transport of pollutants (Mezić et al. (2010); Olascoaga and Haller (2012); Tang and Luna (2013)) or plankton blooms (Bracco et al. (2000); Sandulescu et al. (2007); Rossi et al. (2008); Hernández-Carrasco et al. (2014)). There is an increasing number of eddy resolving data sets available provided either by observations (Donlon et al. (2012)) or by numerical simulations (Thacker et al. (2004); Dong et al. (2009)). Subsequently there is a growing interest in the census of eddies, their size and lifetimes depending on the season. This task requires robust algorithms for the computation of eddy boundaries as well as the precise detection of their appearance and disappearance in time based on numerical velocity fields (Petersen et al. (2013); Wischgoll and Scheuermann (2001); Dong et al. (2014)) as well as altimetry data (Chaigneau et al. (2008); Chelton et al. (2011)). However, the huge amount of available data poses a challenge to data analysis. As pointed out in Chaigneau et al. (2008) mesoscale and submesoscale eddies cannot be extracted from a turbulent flow without a suitable definition and a competitive automatic identification algorithm. Several such algorithms have been developed based on the various concepts mentioned above. In the following we will briefly discuss several of those algorithms.

Based on dynamical systems theory, one can search for Lagrangian coherent structures (LCS) which describe the most repelling or attracting manifolds in a flow (Haller and Yuan (2000)). The time evolution of these invariant manifolds make up the Lagrangian skeleton for the transport of particles in fluid flows. LCS can be considered as the organizing centres of hydrodynamic flows. Their computation is based on the search for stationary curves of shear in case of hyperbolic or parabolic LCS. Elliptic LCS like eddies are computed as stationary curves of averaged strain (Haller and Beron-Vera (2013); Karrasch et al. (2015); Onu et al. (2015)). Other methods to determine whether an eddy can be identified in the flow employ average Lagrangian velocities (Mezić et al. (2010)) or burning invariant manifolds (Mitchell and Mahoney (2012)). The latter have been introduced originally to track fronts in reaction diffusion systems (Mahoney et al. (2012)) but have recently extended to the detection of eddies (Mahoney and Mitchell (2015)). A completely different approach which connects geometric properties of a flow with probabilistic measures utilizes transfer operators to identify LCS (Froyland and Padberg (2009)). Another, more heuristic approach is the computation of distinguished hyperbolic trajectories (DHT) and their stable and unstable manifolds to identify Lagrangian coherent structures in a flow. DHTs can be considered as a generalization of stagnation points of saddle type and their separatrices to general time-dependent flows (Ide et al. (2002); Wiggins (2005); Mancho et al. (2006)). Algorithms to compute DHTs and their manifolds rely on the computation of the ridges of Lagrangian descriptors such as e.g. arc lengths along trajectories of particles in the flow (Mancho et al. (2013)). Stable and unstable manifolds can also be calculated using the ridges of finite time or finite size Lyapunov exponents (FTLE or FSLE) (Artale et al. (1997); Boffetta et al. (2001); d'Ovidio et al. (2004)) using the idea that initially nearby particles in a flow will move apart in stretching regions while they will move closer to each other in contracting regions. The unstable manifolds are often called material lines in 2d (Koh and Legras (2002)) and surfaces in 3d flows (Haller (2001); Bettencourt et al. (2012); Froyland et al. (2012)), since particles would gather along these manifolds identifying them as barriers to transport. While most of the algorithms mentioned above possess the property of objectivity, i.e. they are invariant with respect to certain transformations of the Eulerian coordinate system, the method of Lagrangian descriptors lacks this property (Haller (2015)). Nevertheless, they are often used since the implementation of this



method is easy and the computation is fast. This is particularly important when analysing large velocity fields with lots of LCS appearing and disappearing. Hence, the heuristic method of Lagrangian descriptors is very appealing and might be more appropriate to gain insight into oceanographic flows in a considerable amount of time. It has already been successfully applied to compute Lagrangian coherent structures in the Kuroshio current (Mendoza et al. (2010); Mendoza and Mancho (2010)) and the Polar Vortex (de la Cámara et al. (2012)) as well as analysing the possible dispersion of debris from the Malaysian Airlines flight MH370 airplane in the Indian Ocean (García-Garrido et al. (2015)).

In oceanography, one of the most popular methods to identify eddies is based on the Okubo-Weiss parameter (Okubo (1970); Weiss (1991)). This method relies on the strain and vorticity of the velocity field, and has been applied to both, numerical ocean model output and satellite data (Isern-Fontanet et al. (2006); Chelton et al. (2011)). Often, the underlying velocity field is derived from altimetric data under the assumption of geostrophic theory. In this approach two limitations can appear. First, the derivation of the velocity field can induce noise in the strain and vorticity field. This is usually reduced by applying a smoothing algorithm, which might, in turn, remove physical information. Secondly, Douglass and Richman (2015) show that eddies can have a significant ageostrophic contribution. Thus, the detection might fail when relying on geostrophic theory. A slightly different approach was developed by Yang et al. (2001) and Fernandes et al. (2011), who used the signature of eddies in the sea surface temperature (SST) to detect them. Anyhow, the partially sparse coverage of satellite SST data limits the application of this method.

Sadarjoen and Post (2000) developed a tracking algorithm that is based on the flow geometry. The assumption is that eddies can be defined as features characterized by circular or spiral streamlines around the core of an eddy. The streamlines are derived from the velocity field. Additionally, the change of direction of the segments that compose the streamline (winding angle) is computed for each streamline. Chaigneau et al. (2008) applied this winding angle approach to a data set of the South Pacific. Moreover, they compared the winding angle method to the Okubo-Weiss approach and concluded that the former is more successful in detecting eddies and more important with a much smaller excess of detection errors. A further method based on geometric properties is proposed by Nencioli et al. (2010). The underlying idea is that within an eddy, the velocity field changes its direction in a unique way. Moreover, the relative velocity in the eddy core should vanish and should be enclosed by closed stream lines. This detection and tracking algorithm was successfully applied by Dong et al. (2012) in the Southern California Bight. In addition, the detection algorithm of Nencioli et al. (2010) has the advantage that its application is not limited to surface fields (Isern-Fontanet et al. (2006); Chelton et al. (2011); Fernandes et al. (2011)). Thus, it is possible to track eddies in the interior of the ocean, without any surface signature.

In this paper we develop an eddy detection and tracking tool based on the heuristic method of the Lagrangian descriptor by Mancho and co-workers (Madrid and Mancho (2009); Mancho et al. (2013)). Instead of using the arc length of trajectories we propose to use the modulus of the vorticity as the scalar quantity to be computed along a trajectory. We find this method combining the Eulerian and Lagrangian approaches to be more reliable in the detection of eddies and their lifetimes than other methods. More specifically we compare our method to four others, namely the Lagrangian descriptor using the arc length (Madrid and Mancho (2009); Mendoza et al. (2010)), an oceanographic method based on geometric properties of the flow field (Nencioli et al. (2010)) and detection tools which employ the Okubo-Weiss parameter and the vorticity itself.



The paper is organized as follows: Sect. 2 briefly reviews the Eulerian concepts vorticity and Okubo-Weiss parameter, the Lagrangian descriptor based on the arc length and introduces our Euler-Lagrangian descriptor. To demonstrate the performance of this method compared to the Lagrangian descriptor we use two simple velocity fields: the model of four counter rotating eddies and a modified van Karman vortex street in Sect. 3. In Sect. 4 we describe the implementation of the Euler-Lagrangian descriptor as a tracking tool identifying eddy lifetimes (Sect. 4.1) and compare the results again with the aforementioned other methods. In Sect. 4.2 we study the performance of the method in cases where we corroborate the velocity fields with noise to test the robustness of the method if applied to velocity fields obtained from observational data. Finally in Sect. 4.3 we compare the Eulerian and the Euler-Lagrangian view of the eddy shape with application to the modified van Karman vortex street and to a velocity field which is similar to the one introduced by Abraham (1998) to study the impact of mesoscale hydrodynamic structures on plankton blooms. We conclude the paper with a discussion in Sect.5.

2 From Eulerian and Lagrangian methods to an Euler-Lagrangian method

The dynamics of a fluid can be characterized employing two different concepts: the Eulerian and the Lagrangian view. While the Eulerian view uses quantities describing different properties of the velocity field, the Lagrangian view provides quantities from the perspective of a moving fluid particle. Out of the variety of different Eulerian and Lagrangian methods mentioned in the introduction, we recall here briefly only those concepts, which will be important for our development of a measure to identify eddies in a flow.

An Eulerian method to describe the circulation density of a velocity field in hydrodynamics is vorticity $\mathbf{W}(x, t)$ defined as the curl of the velocity field $\mathbf{v}(x, t)$. The vorticity associates a vector to each point in the fluid representing the local axis of rotation of a fluid particle. It displays areas with a large circulation density like eddies as regions of large vorticity and eddy cores as local maxima.

Another Eulerian quantity is the Okubo-Weiss parameter OW . It weights the strain properties of the flow against the vorticity properties and distinguishes so strain dominated areas from vorticity dominated one. The Okubo-Weiss parameter is defined as

$$OW = s_n^2 + s_s^2 - \omega^2, \quad (1)$$

where the normal strain component s_n , the shear strain component s_s and the relative vorticity ω of a two dimensional velocity field $\mathbf{v} = (u, v)$ are defined as

$$s_n = \frac{\partial u}{\partial x} - \frac{\partial v}{\partial y}, \quad s_s = \frac{\partial v}{\partial x} + \frac{\partial u}{\partial y} \quad \text{and} \quad \omega = \frac{\partial v}{\partial x} - \frac{\partial u}{\partial y}. \quad (2)$$

Eddies are areas having a negative Okubo-Weiss parameter with a local minimum at the eddy core because here the vorticity component outweighs the strain component, while strain dominated areas are characterized by a positive Okubo-Weiss parameter.

A Lagrangian view on the dynamics of the velocity field is given by the Lagrangian descriptor developed by Mancho and



coworkers (Madrid and Mancho (2009)). A more general definition of the Lagrangian descriptor is outlined in Mancho et al. (2013). Here we use the Lagrangian descriptor based on the arc length of a trajectory. It is defined as

$$M(\mathbf{x}^*, t^*)_{v, \tau} = \int_{t^* - \tau}^{t^* + \tau} \sqrt{\sum_{i=1}^n \left(\frac{dx_i(t)}{dt} \right)^2} dt \quad (3)$$

with $\mathbf{x}(t) = (x_1(t), x_2(t) \dots x_n(t))$ being the trajectory of a fluid particle in the velocity field \mathbf{v} that is defined in the time interval $[t^* - \tau, t^* + \tau]$ and going through the point \mathbf{x}^* at time t^* .

The Lagrangian descriptor M can distinguish stable and unstable manifolds as well as hyperbolic and elliptic regions in the velocity field at the same time. The reason is that M accumulates different values of the arc length depending on the dynamics in the region. Trajectories that have a similar dynamical evolution, yield similar values of M . When the dynamics changes abruptly, M will change too. This is the case at fixed points and stable and unstable manifolds. In case of manifolds trajectories on both sides of the manifold have a different behaviour compared to the behaviour of the trajectories on the manifold. Either they approach the manifold very fast or they move away from the manifold very fast. In both cases they accumulate a larger values of M in a given time interval than trajectories on the manifold. Therefore the manifold is displayed as a singular line of M in a contour plot of M . Fixed points themselves correspond to local minima of M . Here the trajectories do not leave the region of the fixed point and accumulate small values of M . As a consequence the Lagrangian descriptor M cannot distinguish between elliptic and hyperbolic fixed points and is therefore not suitable to identify eddies without using a second criterion. Therefore the Eulerian and the Lagrangian view on the dynamics in a flow will be combined into a new quantity.

As already pointed out by Mancho et al. (2013) any intrinsic physical or geometrical property of trajectories can be used to construct a Lagrangian descriptor by integrating this property along trajectories over a certain time interval. Therefore, we introduce a vorticity based Lagrangian descriptor M_V in which the physical quantity is the modulus of the vorticity W of a velocity field $\mathbf{v}(\mathbf{x}, t)$

$$W(\mathbf{x}, t) = |\nabla \times \mathbf{v}(\mathbf{x}, t)|. \quad (4)$$

We define the Euler-Lagrangian descriptor M_V as

$$M_V(\mathbf{x}^*, t^*)_{\tau} = \int_{t^* - \tau}^{t^* + \tau} (W(\mathbf{x}, t))^{\gamma} dt \quad (5)$$

with $\gamma = \frac{1}{2}$. The Euler-Lagrangian descriptor M_V combines the Eulerian and the Lagrangian view of a dynamical system by measuring the Eulerian quantity modulus of vorticity along a trajectory (Lagrangian view) passing through a position \mathbf{x}^* at time t^* in a time interval $[t^* - \tau, t^* + \tau]$. Within this time interval trajectories accumulate different values of M_V . In case of elliptic fixed points, the trajectory does not leave the eddy core but collects large values of modulus of vorticity within this region. Hence, elliptic fixed points are local maxima in the contour plot of M_V . By contrast, hyperbolic fixed points are local minima. Here the trajectories stay in a region of small modulus of vorticity values. The manifolds are lines along which strain dominates and therefore the collected modulus of vorticity along a trajectory is smaller than in regions of different dynamical

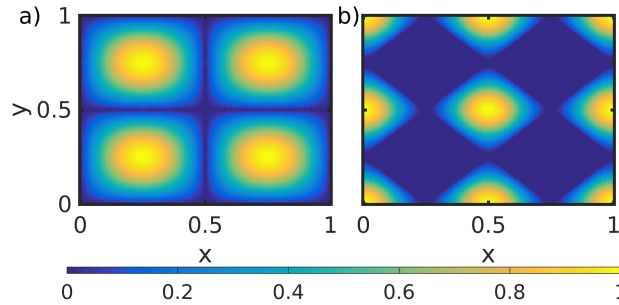


Figure 1. Colour-coded representation of the modulus of vorticity (a), Okubo-Weiss-Parameter (b) for the eddy field in Eq. (6). All plots are normalized to the maximum value.

behaviour. The stable and unstable manifolds are again lines of small M_V .

In case of M_V as well as in case of M the resolution of structures like manifolds and fixed points depends on the choice of the parameter τ that gives the length of the time interval. Structures that live shorter than 2τ cannot be resolved. Even structures that live longer than 2τ can only be resolved if τ is chosen large enough. The choice of τ depends on the structure and the time
 5 scale of the flow field considered. Within the range of the time scale of the problem that should be resolved some variation of τ is needed until the optimal τ for a given problem is found.

3 Eddies in a flow: Comparing the Eulerian, Lagrangian and Euler-Lagrangian methods

To compare the performance of the proposed Euler-Lagrangian method to others two test cases, namely a convection flow consisting of four counter rotating eddies and a model of a vortex street, are used. The four counter rotating eddies are used
 10 to show that different methods detect different aspects of the eddies. Additionally we discuss how the displayed structure depends on the chosen τ . The vortex street is particularly used to test how suitable our method is to detect and track eddies in comparison to other methods and how well they all estimate eddy lifetimes and shapes. This way we gain insight into performance, advantages and disadvantages of the proposed method compared to the others.

To give a complete view of the advantages and disadvantages the results of the different test cases are interpreted in a coherent
 15 discussion after presenting all results.

The equation of motion of fluid particles in a convection flow of four counter rotating eddies are given by

$$u = \dot{x} = \sin(2\pi \cdot x) \cdot \cos(2\pi \cdot y) \quad \text{and} \quad v = \dot{y} = -\cos(2\pi \cdot x) \cdot \sin(2\pi \cdot y). \quad (6)$$

We compute the four different quantities, modulus of vorticity, Okubo-Weiss parameter, Lagrangian descriptor and Euler-Lagrangian descriptor on a spatial domain $(0, 1) \times (0, 1)$. To this end the spatial domain is decomposed into a discrete grid
 20 (201×201) and the different methods are calculated for each grid point. The results are presented in Figs. 1 and 2.

The model of the vortex street consists of two eddies that emerge at two given positions in space, travel a distance L in positive x -direction and fade out. The two eddies are counter rotating. They emerge and die out periodically with a time shift of half

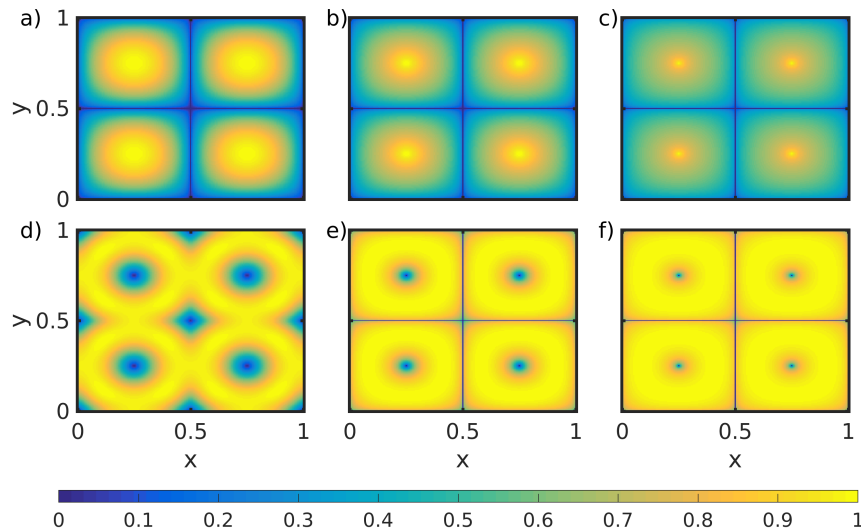


Figure 2. Colour-coded representation of the Euler-Lagrangian descriptor M_V (a-c) and Lagrangian descriptor M (d-f) for the eddy field in Eq. (6) with τ chosen as 0.5 (a and d), 25 (b and e) and 100 (c and f). All plots are normalized to the maximum value.

a period. The model is adapted from Jung et al. (1993) and Sandulescu et al. (2006) with the difference that the cylinder as the cause of eddy formation and its impact on the flow field due to its shade is neglected. In this sense the eddies emerge non-physically out of the blue but all quantities like lifetime and radius to be estimated by means of eddy tracking are then given analytically and make up a perfect test scenario. A detailed description of the model can be found in the supplemental material to this article.

Again all methods are applied to this velocity field using a (302×122) grid. Unless otherwise stated, the time interval τ for the Lagrangian and Euler-Lagrangian methods is set to 0.15 times the lifetime of an eddy. The results are presented in Fig. 3.

These two test cases reveal the following characteristics of the properties of coherent structures in a flow: Eulerian, Lagrangian as well as Euler-Lagrangian methods identify eddy cores (moving elliptic fixed points) as local maxima (modulus of vorticity, M_V) or local minima (Okubo-Weiss, M) of the respective quantity (Fig.1,2,3). The Lagrangian and the Euler-Lagrangian method identify moving hyperbolic fixed points as local minima (Fig. 2e, f). For the Lagrangian descriptor M the centre of the eddy as well as the moving hyperbolic fixed point are indistinguishable since they are both displayed as local minima of M . Our Euler-Lagrangian descriptor M_V can clearly distinguish between the centres of an eddy and moving hyperbolic points (Fig. 2a-c). For this reason Eulerian and Euler-Lagrangian methods are more appropriate than the Lagrangian descriptor M for identifying eddies in a general time-dependent velocity field.

To characterize Lagrangian coherent structures in a flow not only elliptic fixed points associated with eddy cores and moving hyperbolic fixed points have to be identified but also the stable and unstable manifolds associated with the latter to find eddy

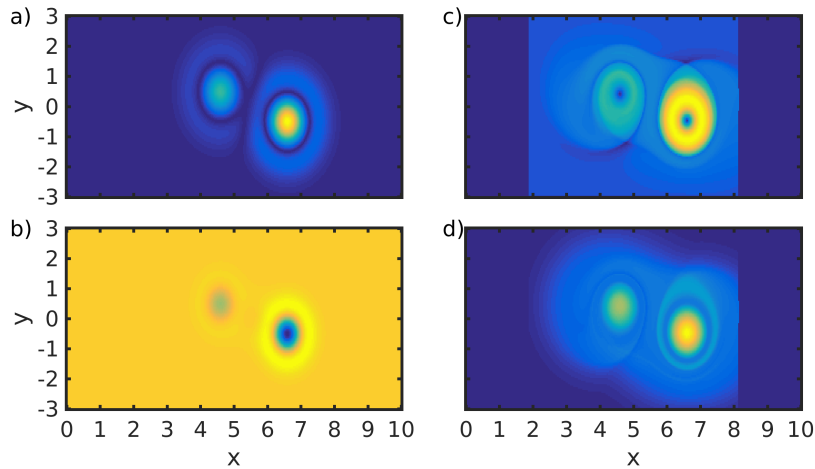


Figure 3. Modulus of vorticity (a), Okubo-Weiss parameter (b), Lagrangian descriptor M (c) and Euler-Lagrangian M_V (d) for the hydrodynamical model of a vortex street at $t = 0.151$ with $\tau = 0.15$, normalized to the maximum value. Blue colours indicate small values yellow large values of the depicted quantity. The dark blue regions in (c) and (d) are regions where the trajectories have left the region of interest.

boundaries. Those manifolds are only identifiable as singular lines in the contour plot using the Lagrangian descriptor M (Fig. 2 d-f, 3 c) and the Euler-Lagrangian descriptor M_V (Fig. 2 a-c, 3 d) respectively.

How detailed the displayed fine structure of the Lagrangian descriptor M and the Euler-Lagrangian descriptor M_V is represented depends on the chosen value of the time interval τ . It ranges from no clear structure for small τ (Fig. 2 a and d) to a detailed structure for large τ (Fig. 2 c and f).

From these properties, distinction elliptic and hyperbolic fixed points and identification of manifolds, we can conclude that the Euler-Lagrangian descriptor M_V is the most suitable quantity to compute when studying oceanographic flows with respect to search for eddies. It is the only quantity of the four quantities considered which allows for a clear identification of eddy cores and the stable and unstable manifolds of hyperbolic fixed points which can be used to get more insight into the size of eddies.

10 For this reason we suggest to use M_V as the basis for an eddy tracking tool.

4 Euler-Lagrangian descriptor M_V as eddy tracking tool

The mean oceanic flow is superimposed by many eddies of different sizes which emerge at some time instant, persist for some time interval and disappear. Consequently, an eddy tracking tool has to detect them at the instance of emergence, track them over their lifetime and detect their disappearance. To classify the different eddies some information about their size is needed

15 too.



In this section we apply the Euler-Lagrangian descriptor M_V to the hydrodynamical model of a vortex street to test its performance as an eddy tracking tool. We use its characteristics that it displays the centres of the eddies (elliptic fixed points) as local maxima and allows simultaneously the identification of invariant manifolds in the flow which in combination with the Lagrangian descriptor M will serve as estimators for the size of the eddies.

5 4.1 Eddy birth and lifetime

We ask how well M_V predicts the lifetime of an eddy and the time instant of the eddy birth and compare the results to the oceanographic eddy tracking tool by Nencioli et al. (2010), as well as Eulerian quantities like the Okubo-Weiss parameter and the modulus of vorticity. As pointed out in the previous section the Lagrangian descriptor M cannot be used as an eddy tracking tool because it does not distinguish between elliptic and hyperbolic fixed points. However, it will be used to determine the size of the eddy, once it has been detected using the Euler-Lagrangian descriptor M_V .

The idea of the tracking inspired by Nencioli et al. (2010) is to search for local maxima (M_V and modulus of vorticity) or local minima (Okubo-Weiss, velocity based method by Nencioli et al. (2010)) surrounded by a region of gradient towards the maximum or minimum in a given search window that is shifted to the region of interest. The size of the search window determines which maximal eddy sizes can be detected. The eddy is tracked from one time step to the other by searching for an eddy core with the same direction of rotation within a given distance. The choice of this distance depends on the velocity field. It should be in the range of the maximal distance a particle could travel in the timespan of interest. The position of an eddy is logged in a track-list for each eddy at each time step. To give a criterion when an eddy track is completed or to avoid false positive tracks or tracks of short living eddies one is not interested in, a threshold number of time steps should be defined. A track-list of an eddy that is not longer updated for this number of time steps is closed. A track-list that is shorter than the threshold number of time steps is deleted. A detailed description of the algorithm can be found in the supplemental material to this article.

In order to check the accuracy of the eddy tracking algorithm, we use the model of the vortex street presented in Sect. 3 in a dimensionless parametrization, since the time instant of birth of the eddies and their lifetimes are given analytically. We measured both quantities for different dimensionless lifetimes T_c and dimensionless vortex strengths of 200, 100 and 50 for the eddy that arises at time $T_c/2$. The rationale behind varying the vortex strength is to estimate how weak an eddy could be to have still a reliable detection by the method. For M_V τ was chosen as $0.15 \cdot T_c$. The results are presented in Figs. 4 and 5.

In all cases independent of the vortex strength, the results obtained with M_V are close to the analytical T_c (Fig. 4) or the analytical time instant of birth (Fig. 5). All other methods underestimate T_c and overestimate the time instant of birth. Especially in case of the eddy tracking tool box (ETTB) by Nencioli et al. (2010) the estimated times depend heavily on the vortex strength. It becomes more and more difficult to detect the eddy as the rotation speed decreases. The reason for the good estimates provided by M_V is that by construction M_V makes use of the history of the eddy (past and future). Hence it can detect eddies earlier than they arise by taking into account the future or detect them longer than they actually exist by looking into the past. M_V is not restricted to the information about the velocity field at one instant of time like the other methods. However, the performance of M_V depends on the chosen value of τ (Fig. 6). If τ gets too large in relation to T_c , the estimate of

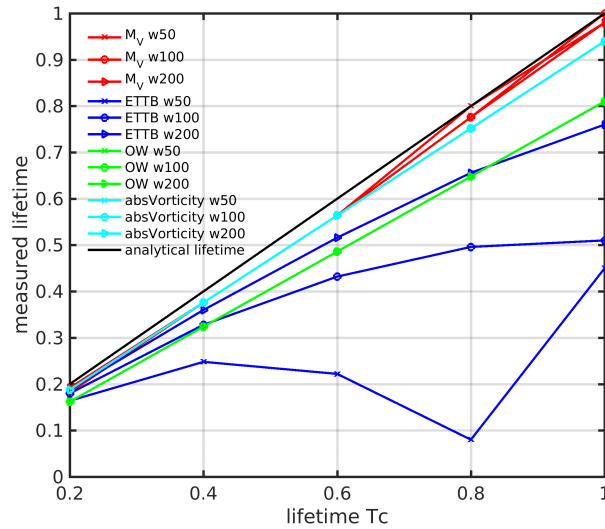


Figure 4. Eddy lifetime estimated with Okubo-Weiss (OW), modulus of vorticity (absVorticity), M_V and the eddy tracking tool box (ETTB) for vortex strength 50, 100 and 200. The black diagonal depicts the analytical lifetime.

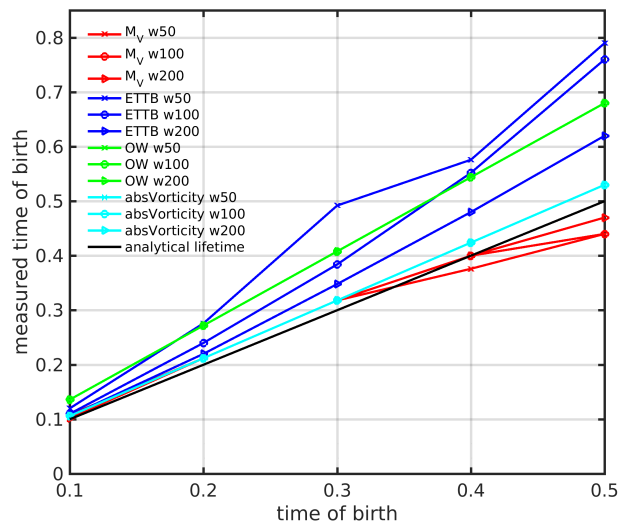


Figure 5. Time of birth of an eddy estimated with Okubo-Weiss (OW), modulus of vorticity (absVorticity), M_V and the eddy tracking tool box (ETTB) for vortex strength 50, 100 and 200. The black diagonal depicts the analytical time of birth of an eddy.

the lifetime deviates from the analytical one because the trajectories contain too much of the history of the eddy. There exists an optimal τ for a certain class of eddies. A good choice in our case is 15 % of the eddy lifetime other application might need a larger or smaller τ .

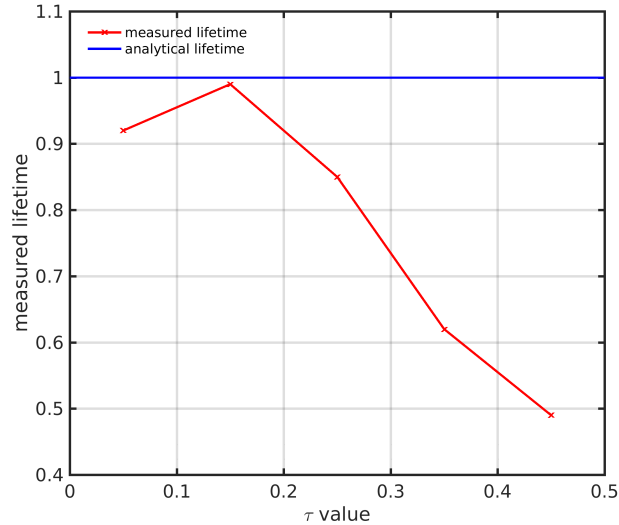


Figure 6. Measured lifetime of an eddy obtained by means of M_V versus the chosen τ (analytical lifetime $T_c = 1$ (blue line), vortex strength 200).

4.2 Robustness of the lifetime detection with respect to noise

Velocity fields describing ocean flows have either a finite resolution when obtained by simulations or contain measurement noise when retrieved from observational data. For this reason an eddy tracking method has to be robust with respect to fluctuations of the velocity field. For this reason we will explore how the detected eddy lifetime depends on noise in the velocity data.

- 5 We use three types of noise based on the different sources of noise that can arise in observations or simulations. The noise level is given dimensionless, because the noise is applied to the dimensionless model of the vortex street presented in Sect. 3.
1. type 1: We add white Gaussian noise of different noise strength between 0.05 and 0.95 to the velocity field of the vortex street with analytical eddy lifetime $T_c = 1$ and vortex strength $w = 200$. The noise is uncorrelated in space and time. The velocity field in this case is still periodic but noisy. This type of noise mimics the effect of computing derivatives of
 10 observed velocity fields (e.g. by satellites or HF-radar).
 2. type 2: We add multiplicative white Gaussian noise of different noise strength between 0.05 and 0.95 to the velocity field of the vortex street. The motivation is that the strength of noise depends on the "Signal to noise" ratio. If we have a strong current, it is easy to detect this by a satellite, since the signal-strength is high. This is opposite for slow currents, where the noise level is much higher. Thus, we add white noise that is inversely proportional to the current speed in the
 15 sense of $\text{noise}/(1+\text{maximum of the current speed})$.
 3. type 3: We add white Gaussian noise of different noise strength between 0.05 and 0.5 to the y -component of the eddy centres' movement. This type of noise can be observed if the velocity fields have to rely on georeferencing. For instance

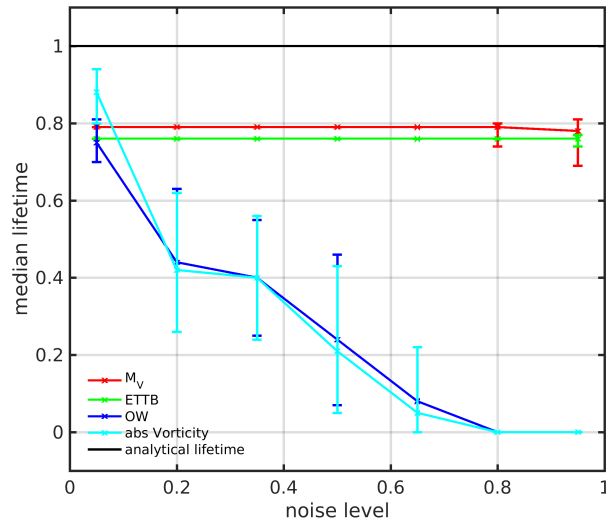


Figure 7. Measured median lifetime obtained by different methods (Okubo-Weiss (OW), modulus of vorticity (absVorticity), M_V and the eddy tracking tool box (ETT)) depending on the noise level. The computations have been performed in a velocity field mimicking a vortex street with added white Gaussian noise (type 1 noise with 1000 noise realizations). The errorbars indicate the whiskers of the distribution in the boxplot (not shown here) corresponding to approximately $\pm 2.7\sigma$.

satellite generated velocity fields have to be mapped on a longitude/latitude grid, since the satellite is moving. During this postprocessing step a shift in the georeference is possible, leading to translational shifts and thus to type 3 noise. However, a high noise level of type 3 is not very likely. If one deals with typical geophysical applications, which have a grid resolution of the order 1 to 10 km, the georeferencing errors are mostly small compared to the grid cell size.

5 We have applied noise of type 1, 2 and 3 to the dimensionless model of the vortex street presented in Sect. 3. We have used 1000 realizations of the white Gaussian noise per noise strength and estimated the lifetime of each eddy that undergoes a whole life-cycle within the time of simulation. The plotted eddy lifetimes obtained with all different tracking methods are medians of the distributions (Fig. 7, 8, 9).

The three types of noise illustrate different advantages and disadvantages of M_V compared to the other methods. In case of
 10 type 1 noise, M_V gives the best estimate of the lifetime compared to the other methods independent of the increasing noise level. The reason why the error of the estimate in case of M_V does not increase with increasing noise level is that M_V is a measure that is based on an integral. It accumulates the uncorrelated noise along the trajectory from past to future. Integrating over this accumulated noise can be considered as a smoothing process. Also the method by Nencioli et al. (2010) gives a good result independent of the increasing noise level, because the signal to noise ratio is small. The minimum of the velocity that
 15 is the key-signal for determining the eddy core in their method is still a local minimum in the contour plot of the velocity. However, with increasing noise level we see an increase of outliers for the method by Nencioli et al. (2010) and M_V (boxplot not shown here) of the data of the method. The performance of modulus of vorticity and the Okubo-Weiss parameter decreases

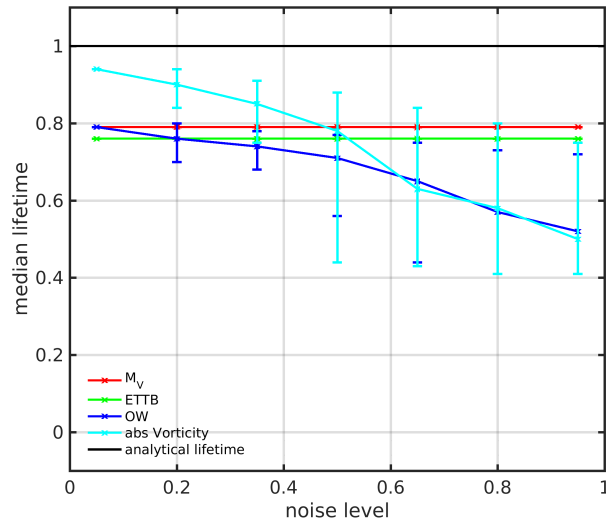


Figure 8. Measured median lifetime obtained by different methods (Okubo-Weiss (OW), modulus of vorticity (absVorticity), M_V and the eddy tracking tool box (ETT)) depending on the noise level. The computations have been performed in a velocity field mimicking a vortex street with type 2 noise (1000 noise realizations). The errorbars indicate the whiskers of the distribution in the boxplot (not shown here) corresponding to approximately $\pm 2.7\sigma$.

as expected with increasing noise level while the distribution increases in width (Fig. 7). The reason is that the noise gets so large that it increasingly disturbs the key-signal for an eddy core until no distinct eddy core can be identified anymore.

In case of type 2 noise, M_V and the method by Nencioli et al. (2010) show a similar behaviour as in case of type 1 noise. Both yield good results independent of the noise level. The modulus of vorticity gives results that are even better than M_V in case of small noise levels, but its performance drops below the results of M_V with increasing noise level (Fig. 8). The reason is that the key-signal for determining an eddy core using the modulus vorticity is stronger in case of small noise levels and gets disturbed by the noise with increasing noise level. By contrast, the smoothing process in M_V is the same independent of the noise level. As expected the performance of Okubo-Weiss decreases with increasing noise level. In contrast to type 1 noise, even in case of strong noise eddy cores can be identified because the key-signal for an eddy core is less disturbed.

10 In case of type 3 noise, M_V yields an estimate of the lifetime with the largest error (Fig. 9). The reason is that in this case noisy trajectories that start close to each other diverge fast, while the ones with no noise have a similar dynamical evolution. This divergence due to noise leads to a loss of structure in space which can be interpreted as a weakening of the correlation between neighbouring trajectories. This effect is strongest in case of M_V because it integrates over time and so neighbouring trajectories that have similar values of M_V in case of no noise yield very different values of M_V due to the divergence of the trajectories. As a consequence no clear structure in M_V can be identified. This effect increases with the noise level.

Also for the other methods noise of type 3 affects the identification of the eddy core because the weakening of the correlation between neighbouring points disturbs the key-signal of an eddy core (a local minimum or maximum in a certain domain). The

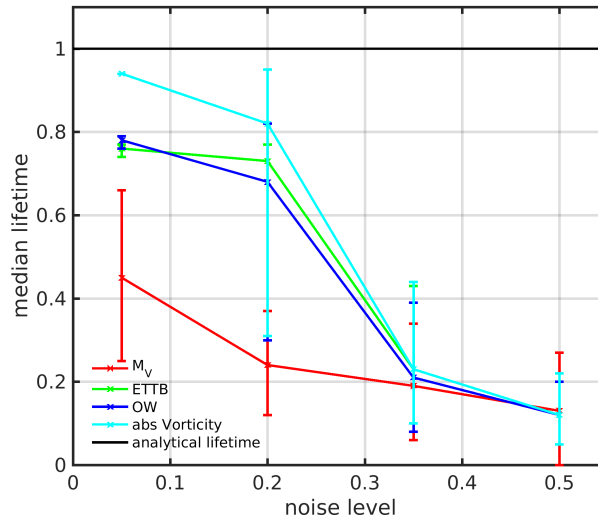


Figure 9. Measured median lifetime obtained by different methods (Okubo-Weiss (OW), modulus of vorticity (absVorticity), M_V and the eddy tracking tool box (ETT)) on the noise level. The computations have been performed in a velocity field mimicking a vortex street with type 3 noise (1000 noise realizations). The errorbars indicate the whiskers of the distribution in the boxplot (not shown here) corresponding to approximately $\pm 2.7\sigma$.

error in estimating the lifetime increases with increasing noise level. In all cases the number of outliers in the boxplot (not shown here) increases with the noise level.

As a result, non of the methods performs in an optimal way when the noise affects the movement of the eddy cores. This disadvantage will lead to deviations in the lifetime statistics for eddy tracking based on observational data. However nowadays, the error in georeferencing of satellite images (which is mimicked by type 3 noise) is mostly small. For special applications, a georeferencing error of smaller than 1/50 pixel is achievable (Leprince et al. (2007)). Eugenio and Marqués (2003) show that with reasonable effort a mapping error smaller than 0.5 pixel is possible, if fixed landmarks (coastlines, islands) are on the images. With the increase in earth orbiting satellites and thus the increase in available images, it can be assumed that this error will drop even more (Morrow and Le Traon (2012)). Anyhow, noise of type 3 is completely absent, if numerically generated velocity fields are used. Here the evolution of neighbouring trajectories are smooth and correlated.

In summary, M_V can be used for the detection of eddies and the estimate of eddy lifetimes for velocity fields with and without noise and yields good results independent of the noise level in case of type 1 and 2 noise. However one has to take into account that the velocity field should not be too noisy and that one has to chose a τ that fits the problem. The Euler-Lagrangian descriptor M_V has an additional advantage in detecting arising eddies earlier than other methods due to collecting information along the trajectory from past to future. This can be useful in the identification of regions that will be eddy dominated in the further evolution of the flow.

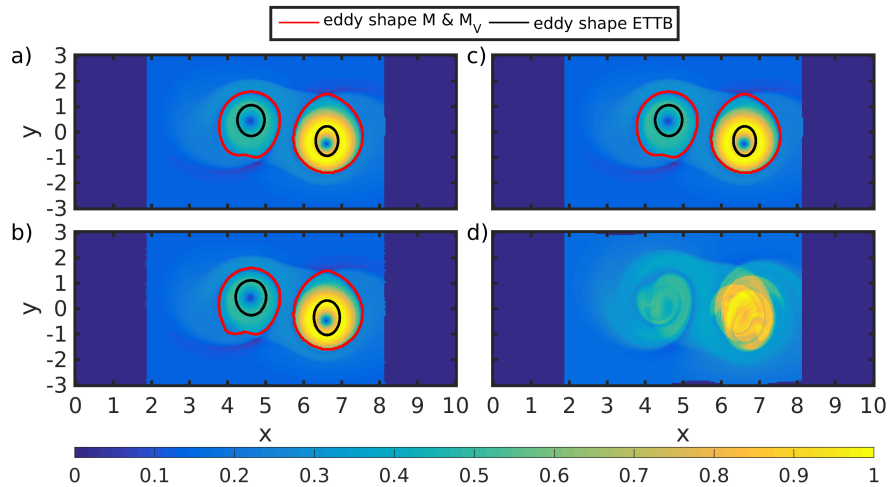


Figure 10. Eddy shape detected with the method based on M and M_V (red line) and with the eddy tracking tool by Nencioli et al. (2010) (black line) at $t = 0.151$. The color code indicates: (a) M , (b) M with type 1 noise of noise level 0.95, (c) M with type 2 noise of noise level 0.95, (d) M with type 3 noise of noise level 0.5. The τ value is chosen as $0.15 T_c$ with $T_c = 1$. The dark blue regions are regions where the trajectories have left the region of interest. All plots are normalized to the maximum value.

4.3 Detecting eddy shapes

Beside its lifetime an eddy is characterized by its shape. In the following we will estimate the eddy shape using a combination of the vorticity-based Euler-Lagrangian M_V and the arc-length based Lagrangian approach M . We compare the results to the shapes detected by the eddy tracking tool by Nencioli et al. (2010). In this way we demonstrate the differences between the

5 Eulerian and Euler-Lagrangian point of view on the eddy shape.

From the Euler-Lagrangian point of view the estimation of the eddy shape is based on the idea that the boundaries of the eddy are linked to manifolds that surround the eddy. This idea has been formulated by Bettencourt et al. (2012), who point out, that eddies are bounded by invariant manifolds surrounding the eddy and acting as transport barriers. These manifolds cannot be crossed by any trajectories and, therefore, trajectories starting inside the manifolds are trapped in the eddy. Defining the

10 boundaries in this way one can estimate the trapping region or volume that is transported by an eddy.

The shape detection algorithm combines the Lagrangian descriptor M and the Euler-Lagrangian descriptor M_V and searches for largest closed contour lines with the local lowest level of M which surrounds the elliptic fixed point found with M_V . This line is a line on or close to the manifold displayed by M or M_V . By contrast, the eddy tracking tool by Nencioli et al. (2010) gives an Eulerian view on the eddy shape by defining the eddy boundaries as the largest closed streamline of the streamfunction

15 around the eddy centre where the velocity still increases radially from the centre.

The comparison of the different views on the eddy shape is presented in Fig. 10 for the vortex street without (a) and with noise of type 1, 2 and 3 (b-d). As expected the shape detected with the eddy tracking tool by Nencioli et al. (2010) is much smaller

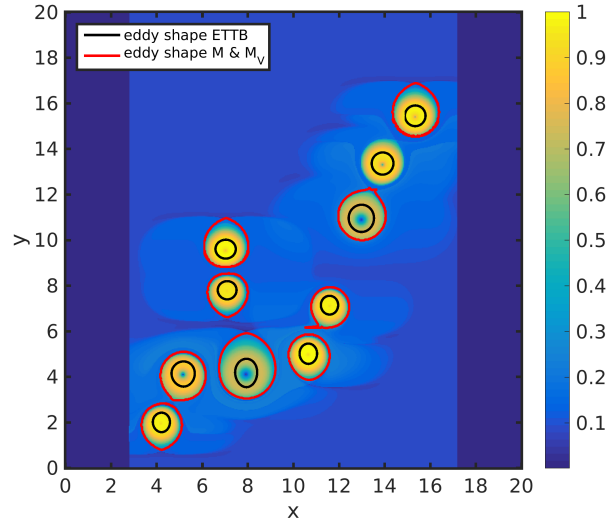


Figure 11. M normalized to the maximum value with the eddy shapes of the seeded eddy model detected with the method based on M and M_V (red lines) and with the eddy tracking tool by Nencioli et al. (2010) (black line). τ is chosen as $0.15 T_c$ with $T_c = 1$. The dark blue regions are regions where the trajectories have left the region of interest.

than the shape based on the Euler-Lagrangian view (Fig. 10 a-c). Additionally the evolution of the eddy is captured by both methods even in case of strong type 1 and 2 noise (Fig. 10 b and c). The shape computed by the combination of M and M_V is detected earlier and shows more growing and shrinking during the evolution of the eddy due to the conceptual idea of the measure that contains the history of the trajectories. As shown in Sect. 4.2 this concept of M and M_V leads to problems in case of a velocity field with type 3 noise (although significant type 3 noise levels are very unlikely). If the noise level is too large no structure can be detected (Fig. 10 d) with M and M_V .

In a real oceanic flow eddies of different lifetime and shape will occur simultaneously. To illustrate how different eddy shapes and sizes can be detected we apply our approach to a seeded eddy model that mimics such an oceanic eddy field. The model is inspired by the seeded eddy model of a turbulent flow described in Abraham (1998) and the model of Jung et al. (1993) to elucidate the role of eddies in the formation of plankton patchiness.

The model consist of a background flow of 0.18 ms^{-1} and ten mesoscale eddies of different sizes. Their radii r are drawn from a distribution possessing a power law $1/r^3$ where the minimal radius is 10 km and the maximal radius is 50 km. Because we are interested in mesoscale eddies, the drawn radii are between 15 km and 25 km. One half of the eddies rotates clockwise and the other half counter-clockwise. Their position in space is drawn from an uniform distribution. To generate a dimensionless model, lengths are measured in units of the maximal eddy radius of the mesoscale eddies and time in units of the lifetime of an eddy which is chosen equally for all eddies ($T_c = 1$). τ is chosen as 0.15. A detailed description can be found in the supplemental material to this article.

The result is presented in Fig. 11. As expected the eddy shapes are larger in case of M and M_V than in case of the eddy



tracking tool by Nencioli et al. (2010) since both approaches use different definitions of the eddy shape. A problem arises in case of M and M_V if the eddy boundaries are too close to each other (Fig. 11 upper right eddies). The eddy tracking based on M_V detects the eddy cores and identifies the eddies as separated. However the filaments of the eddy boundary of one eddy are close to the boundary of the other eddy. The criterion to identify an eddy boundary is to detect the largest closed contour line with the local lowest level of M within a search window. If the boundaries are close to each other any lowest local level of M within the search window can be clearly identified. However, note that this test case is rather artificial. Eddies are placed randomly in the ocean and eddy-eddy interaction is not taken into account. In realistic applications, if eddies are too close to each other, they certainly will interact, merge, or repel each other. Hence, the eddy tracking algorithm might still give reliable results.

In summary, the method based on the combination of the Lagrangian descriptor M and the Euler-Lagrangian descriptor M_V can be used for the detection of eddy boundaries that are acting as boundaries of a trapping region. Comparing the latter to boundaries detected with the method by Nencioli et al. (2010) leads to large differences in the shape computed by both methods. Those differences are due to the difference in the definition of the boundary and yields much smaller sizes of the eddies in case of the eddy tracking tool by Nencioli et al. (2010). Another advantage of the method based on the combination of the Lagrangian descriptor M and the Euler-Lagrangian descriptor M_V is that it even shows filament structures of the eddy boundary in contrast to the method by Nencioli et al. (2010). These filaments can be linked to the dynamics of the eddy, e.g. as it starts interacting, merging, or repelling with other eddies or fading out. Nevertheless one has to take into account that the detection of eddy shapes by the method based on the combination of the Lagrangian descriptor M and the Euler-Lagrangian descriptor M_V is restricted by the unlikely case of type 3 noise in velocity fields.

5 Discussion and conclusion

We have shown, that the introduced heuristic Euler-Lagrangian descriptor M_V provides a good insight in the flow structure of a hydrodynamic system. It identifies elliptic fixed points that can be linked to eddy cores and, in contrast to Eulerian measures, M_V even identifies hyperbolic fixed points. Moreover it can distinguish between elliptic and hyperbolic fixed points - a property which cannot be achieved by the Lagrangian descriptor M . Therefore, the Euler-Lagrangian descriptor M_V is a suitable tool for tracking eddies and subsequently estimating their lifetimes. Like the Lagrangian descriptor M , M_V displays the stable and unstable manifolds and provides as an add-on estimates of the eddy boundaries. This fact linked to the idea that manifolds cannot be crossed by trajectories yields a different approach to the tracking of eddy shapes compared to an Eulerian method. Eulerian methods like the one of Nencioli et al. (2010) define the eddy boundary as a line with special properties of the velocity which cannot be linked to the idea of trapping of fluid parcels inside the eddy.

We have demonstrated using some paradigmatic velocity fields that the proposed Euler-Lagrangian descriptor M_V yields good results in estimating the lifetimes of eddies and in combination with the Lagrangian descriptor M eddy shapes. Therefore, it is a suitable tool for eddy tracking in oceanic velocity fields. The Euler-Lagrangian descriptor M_V gives an estimate of the lifetime that is closest to the analytical lifetime (in the case of the vortex street), therefore it performs much better than any of



the other methods in the comparison. It finds eddies earlier than the other methods because M_V contains information of the future and the past of the velocity field. This property can be useful if one is interested in the process of the eddy birth and its early evolution. However, there are some disadvantages of this method which need to be addressed.

First of all, it is a heuristic method, that lacks objectivity. This can be problematic since it might lead to failures in the detection of some eddies. But it is easy to implement and fast, so that it compensates for this problem, when this measure is used for computing census and size distributions of eddies in oceanic flows over a long period of time. A general problem of the Lagrangian and the Euler-Lagrangian descriptors is that the resolution of the structures to be detected depends on the chosen time τ . Structures that live too short in relation to the chosen τ cannot be resolved and will be missed. Hence the choice of τ contains a decision which time scale and subsequently which eddy lifetime will be resolved. We have shown that the Euler-Lagrangian descriptor M_V provides still good results if the velocity field is corroborated with noise of type 1 and 2. This is due to the smoothing effect inherent in the definition of M_V as an integral along the trajectory. The estimates of the eddy lifetime by M_V is in almost all cases better than the estimate of the other methods. In case of velocity fields with strong type 3 noise collecting the history of the velocity field can be a drawback. As discussed in Sect. 4.2 type 3 noise leads to a divergence of neighbouring trajectories, which disturbs the structure of M_V and in this way the detection of the eddy core or shape. A solution for this problem is the choice of a smaller time τ to reduce the time span where the trajectories can diverge from each other. However, as discussed in Sect. 4.2 type 3 noise is very unlikely and completely absent, if numerical generated velocity fields are used.

In general, the choice of the detection method depends on the questions asked. If one is only interested in tracking eddy cores Eulerian methods are a good choice. Lagrangian and especially the Euler-Lagrangian method gives a more detailed view on the dynamics. Besides, they provide a more physical estimate of the eddy size. Especially this feature, which describes the fluid volume trapped in an eddy promises to be more useful for applications that consider the growth of plankton populations in oceanic flows. For the latter it has been shown that eddies can act as incubators for plankton blooms due to the confinement of plankton inside the eddy (Oschlies and Garçon (1999); Martin (2003); Sandulescu et al. (2007)).

Author contributions. Rahel Vortmeyer-Kley developed the idea of the Euler-Lagrangian descriptor and implemented the eddy tracking tool based on it. Ulf Gräwe supervised the oceanic questions of this work. The overall supervision was done by Ulrike Feudel. All authors contributed in preparing this manuscript.

Acknowledgements. Rahel Vortmeyer-Kley would like to thank the Studienstiftung des Deutschen Volkes for a doctoral fellowship. The financing of further developments of the Leibniz Institute of Baltic Sea Research monitoring program and adaptations of numerical models (STB-MODAT) by the federal state government of Mecklenburg-Vorpommern is greatly acknowledged by Ulf Gräwe.

The authors would like to thank Jan Freund, Wenbo Tang and Tamás Tél for stimulating discussions.



References

- Abraham, E. R.: The generation of plankton patchiness by turbulent stirring, *Nature*, 391, 577–580, 1998.
- Artale, V., Boffetta, G., Celani, M., Cencini, M., and Vulpiani, A.: Dispersion of passive tracers in closed basins: Beyond the diffusion coefficient, *Phys Fluids*, 9, 3162–3171, 1997.
- 5 Bastine, D. and Feudel, U.: Inhomogeneous dominance patterns of competing phytoplankton groups in the wake of an island, *Nonlinear Proc Geoph*, 17, 715–731, 2010.
- Bettencourt, J. H., López, C., and Hernández-García, E.: Oceanic three-dimensional Lagrangian coherent structures: A study of a mesoscale eddy in the Benguela upwelling region, *Ocean Model*, 51, 73–83, 2012.
- Boffetta, G. and Lacorata, G., Redaelli, G., and Vulpiani, A.: Detecting barriers to transport: a review of different techniques, *Physica D*, 159, 58–70, 2001.
- 10 Bracco, A., Provenzale, A., and Scheuring, I.: Mesoscale vortices and the paradox of the plankton, *P Roy Soc Lond B Bio*, 267, 1795–1800, 2000.
- Chaigneau, A., Gizolme, A., and Grados, C.: Mesoscale eddies off Peru in altimeter records: Identification algorithms and eddy spatio-temporal patterns, *Prog Oceanogr*, 79, 106–119, 2008.
- 15 Chelton, D. B., Schlax, M. G., and Samelson, R. M.: Global observations of nonlinear mesoscale eddies, *Prog Oceanogr*, 91, 167–216, 2011.
- de la Cámara, A., Mancho, A. M., Ide, K., Serrano, E., and Mechoso, C. R.: Routes of Transport across the Antarctic Polar Vortex in the Southern Spring, *J Atmos Sci*, 69, 741–752, 2012.
- Dong, C., Idica, E. Y., and McWilliams, J. C.: Circulation and multiple-scale variability in the Southern California Bight, *Prog Oceanogr*, 82, 168–190, 2009.
- 20 Dong, C., Lin, X., Liu, Y., Nencioli, F., Chao, Y., Guan, Y., Chen, D., Dickey, T., and McWilliams, J. C.: Three-dimensional oceanic eddy analysis in the Southern California Bight from a numerical product, *J Geophys Res*, 117, C00H14, 2012.
- Dong, C., McWilliams, J. C., Liu, Y., and Chen, D.: Global heat and salt transports by eddy movement, *Nature Communications*, 5, 1–6, 2014.
- Donlon, C. J., Martin, M., Stark, J., Roberts-Jones, J., Fiedler, E., and Wimmer, W.: The Operational Sea Surface Temperature and Sea Ice Analysis (OSTIA) system, *Remote Sensing of Environment*, 116, 140–158, 2012.
- 25 Douglass, E. M. and Richman, J. G.: Analysis of ageostrophy in strong surface eddies in the Atlantic Ocean, *J Geophys Res: Oceans*, 120, 1490–1507, 2015.
- d’Ovidio, F., Fernández, V., Hernández-García, E., and López, C.: Mixing structures in the Mediterranean Sea from Finite-Size Lyapunov Exponents, *Geophys Res Lett*, 31, L17203, 2004.
- 30 Eugenio, F. and Marqués, F.: Automatic Satellite Image Georeferencing Using a Contour-Matching Approach, *IEEE T Geosci Remote*, 41, 2869–2880, 2003.
- Fernandes, M. A., Nascimento, S., and Boutov, D.: Automatic identification of oceanic eddies in infrared satellite images, *Comput Geosci*, 37, 1783–1792, 2011.
- Froyland, G. and Padberg, K.: Almost-invariant sets and invariant manifolds - Connecting probabilistic and geometric descriptions of coherent structures in flows, *Physica D*, 238, 1507–1523, 2009.
- 35 Froyland, G., Horenkamp, C., Rossi, V., Santitissadeekorn, N., and Guptac, A. S.: Three-dimensional characterization and tracking of an Agulhas Ring, *Ocean Model*, 52, 69–75, 2012.



- García-Garrido, V., Mancho, A. M., Wiggins, S., and Mendoza, C.: A dynamical systems approach to the surface search for debris associated with the disappearance of flight MH370, *Nonlinear Proc Geoph*, 22, 701–712, 2015.
- Gawlik, E. S., Marsden, J. E., Du Toit, P. C., and Campagnola, S.: Lagrangian coherent structures in the planar elliptic restricted three-body problem, *Celest Mech Dyn Astr*, 103, 227–249, 2009.
- 5 Haller, G.: Distinguished material surfaces and coherent structures in three-dimensional fluid flows, *Physica D*, 149, 248–277, 2001.
- Haller, G.: Lagrangian Coherent Structures, *Annu Rev Fluid Mech*, 47, 137–162, 2015.
- Haller, G. and Beron-Vera, F.: Coherent Lagrangian vortices: the black holes of turbulence, *J Fluid Mech*, 731, R4, 2013.
- Haller, G. and Yuan, G.: Lagrangian coherent structures and mixing in two-dimensional turbulence, *Physica D*, 147, 352–370, 2000.
- Hernández-Carrasco, I., Rossi, V., Hernández-García, E., Garçon, V., and López, C.: The reduction of plankton biomass induced by mesoscale
10 stirring: A modeling study in the Benguela upwelling, *Deep-Sea Res Pt I*, 83, 65–80, 2014.
- Huhn, F., Kameke, A., Pérez-Muñuzuri, V., Olascoaga, M., and Beron-Vera, F.: The impact of advective transport by the South Indian Ocean Countercurrent on the Madagascar plankton bloom, *Geophys Res Lett*, 39, 2012.
- Ide, K., Small, D., and Wiggins, S.: Distinguished hyperbolic trajectories in time-dependent fluid flows: analytical and computational approach for velocity fields defined as data sets, *Nonlinear Proc Geoph*, 9, 237–263, 2002.
- 15 Isern-Fontanet, J., García-Ladona, E., and Font, J.: Vortices of the Mediterranean Sea: An Altimetric Perspective, *J Phys Oceanogr*, 36, 87–103, 2006.
- Jung, C., Tél, T., and Ziemniak, E.: Application of scattering chaos to particle transport in a hydrodynamical flow, *Chaos*, 3, 555–568, 1993.
- Karrasch, D., Huhn, F., and Haller, G.: Automated detection of coherent Lagrangian vortices in two-dimensional unsteady flows, *P Roy Soc A - Math Phy*, 471, 20140 639, 2015.
- 20 Koh, T. Y. and Legras, B.: Hyperbolic lines and the stratospheric polar vortex, *Chaos*, 12, 382–394, 2002.
- Leprieux, S., Barbot, S., Ayoub, F., and Avouac, J. P.: Automatic and precise orthorectification, coregistration, and subpixel correlation of satellite images, application to ground deformation measurements, *IEEE T Geosci Remote*, 45, 1529–1558, 2007.
- Madrid, J. A. J. and Mancho, A. M.: Distinguished trajectories in time dependent vector fields, *Chaos*, 19, 013 111–1–18, 2009.
- Mahoney, J., Bargteil, D., Kingsbury, M., Mitchell, K., and Solomon, T.: Invariant barriers to reactive front propagation in fluid flows,
25 *Europhys Lett*, 98, 44 005, 2012.
- Mahoney, J. R. and Mitchell, K. A.: Finite-time barriers to front propagation in two-dimensional fluid flows, *Chaos*, 25, 087 404–1–10, 2015.
- Mancho, A., Small, D., and Wiggins, S.: A tutorial on dynamical systems concepts applied to Lagrangian transport in oceanic flows defined as finite time data sets: Theoretical and computational issues, *Phy Rep*, 437, 55–124, 2006.
- Mancho, A., Wiggins, S., Curbelo, J., and Mendoza, C.: Lagrangian Descriptors: A method of revealing phase space structures of general
30 time dependent dynamical systems, *Commun Nonlinear Sci*, 18, 3530–3557, 2013.
- Martin, A.: Phytoplakton patchiness: the role of lateral stirring and mixing, *Prog Oceanogr*, 57, 125–174, 2003.
- Martin, A., Richards, K., Bracco, A., and Provenzale, A.: Patchy productivity in the open ocean, *Global Biogeochem Cy*, 16, 9–1, 2002.
- Mendoza, C. and Mancho, A.: Hidden geometry of ocean flows, *Phys Rev Lett*, 105, 038 501–1–4, 2010.
- Mendoza, C., Mancho, A., and Rio, M.-H.: The turnstile mechanism across the Kuroshio current: analysis of the dynamics in altimeter
35 velocity fields, *Nonlinear Proc Geoph*, 17, 103–111, 2010.
- Mezić, I., Loire, S., Fonoberov, V. A., and Hogan, P.: A New Mixing Diagnostic and Gulf Oil Spill Movement, *Science*, 330, 486–489, 2010.
- Mitchell, K. A. and Mahoney, J. R.: Invariant manifolds and the geometry of front propagation in fluid flows, *Chaos*, 22, 037 104–1–13, 2012.



- Morrow, R. and Le Traon, P.-Y.: Recent advances in observing mesoscale ocean dynamics with satellite altimetry, *Adv Space Res*, 50, 1062–1076, 2012.
- Nencioli, F., Dong, C., Dickey, T., Washburn, L., and McWilliams, J. C.: A Vector Geometry-Based Eddy Detection Algorithm and Its Application to a High-Resolution Numerical Model Product and High-Frequency Radar Surface Velocities in the Southern California Bight, *J Atmos Ocean Tech*, 27, 564–579, 2010.
- Okubo, A.: Horizontal dispersion of floatable particles in the vicinity of velocity singularities such as convergences, *Deep Sea Research and Oceanographic Abstracts*, 17, 445–454, 1970.
- Olascoaga, M. J. and Haller, G.: Forecasting sudden changes in environmental pollution patterns, *PNAS*, 109, 4738–4743, 2012.
- Onu, K., Huhn, F., and Haller, G.: LCS Tool: A Computational Platform for Lagrangian Coherent Structures, *Journal of Computational Science*, 7, 26–36, 2015.
- Oschlies, A. and Garçon, V.: An eddy-permitting coupled physical-biological model of the North-Atlantic, sensitivity to advection numerics and mixed layer physics, *Global Biogeochem Cy*, 13, 135–160, 1999.
- Petersen, M. R., Williams, S. J., Maltrud, M. E., Hecht, M. W., and Hamann, B.: A three-dimensional eddy census of a high-resolution global ocean simulation, *J Geophys Res: Oceans*, 118, 1759–1774, 2013.
- Rossi, V., López, C., Sudre, J., Hernández-García, E., and Garçon, V.: Comparative study of mixing and biological activity of the Benguela and Canary upwelling systems, *Geophys Res Lett*, 35, 2008.
- Sadarjoen, I. A. and Post, F. H.: Detection, quantification, and tracking of vortices using streamline geometry, *Comput Graph*, 24, 333–341, 2000.
- Sandulescu, M., Hernández-García, E., López, C., and Feudel, U.: Kinematic studies of transport across an island wake, with application to Canary islands, *Tellus A*, 58, 605–615, 2006.
- Sandulescu, M., López, C., Hernández-García, E., and Feudel, U.: Plankton blooms in vortices: the role of biological and hydrodynamic timescales, *Nonlinear Proc Geoph*, 14, 443–454, 2007.
- Tang, W. and Luna, C.: Dependence of advection-diffusion-reaction on flow coherent structures, *Phys Fluids*, 25, 106 602–1–19, 2013.
- Thacker, W. C., Lee, S.-K., and Halliwell, G. R.: Assimilating 20 years of Atlantic XBT data into HYCOM: a first look, *Ocean Model*, 7, 183–210, 2004.
- Weiss, J.: The dynamics of enstrophy transfer in two-dimensional hydrodynamics, *Physica D: Nonlinear Phenomena*, 48, 273–294, 1991.
- Wiggins, S.: The dynamical systems approach to Lagrangian transport in oceanic flows, *Annu Rev Fluid Mech*, 37, 295–328, 2005.
- Wilson, M. M., Peng, J., Dabiri, J. O., and Eldredge, J. D.: Lagrangian coherent structures in low Reynolds number swimming, *J Phys-Condens Mat*, 21, 204 105, 2009.
- Wischgoll, T. and Scheuermann, G.: Detection and visualization of closed streamlines in planar flows, *IEEE T Vis Compu Gr*, 7, 165–172, 2001.
- Yang, Q., Parvin, B., and Mariano, A.: Detection of vortices and saddle points in SST data, *Geophys Res Lett*, 28, 331–334, 2001.